ORIGINAL RESEARCH PAPER
Volume - 11 | Issue - 06 | June - 2022 | PRINT ISSN No. 2277 - 8179 | DOI : 10.36106/ijsr
INTERNATIONAL JOURNAL OF SCIENTIFIC RESEARCH

TARGETING EGFR $^{L858R/T790M/C797S}$ ALLOSTERIC SITES FOR NSCLC THERAPY: MOLECULES WITH NOVEL MULTI-KINASE BINDING POTENTIAL

Biology

Dr. Kavita Kumari Kakarala* Bhagwan Mahavir Medical Research Centre. 10-1-1, Mahavir Marg, AC Guards, Lakdikapul, Hyderabad, Telangana 500004, India. *Corresponding Author

Dr. Kaiser Jamil Bhagwan Mahavir Medical Research Centre. 10-1-1, Mahavir Marg, AC Guards, Lakdikapul, Hyderabad, Telangana 500004, India.

ABSTRACT

EGFR is the most promising therapeutic target for non-small cell lung cancer (NSCLC). The high rate of mortality fuelled by drug resistance and toxic side effects led to the development of allosteric drugs targeting EGFR, as an alternative treatment option for NSCLC patients. Despite the benefits of allosteric drugs, long-term treatment was impeded by low oral bioavailability and drug accumulation, putting NSCLC patients' life expectancies in jeopardy. In this study, the active molecules with established activity against network kinases were studied using computational methods to identify potential drug-like allosteric inhibitors of EGFR L858R/T790M/C797S with multi-kinase inhibition potential. The computational methodology included: 1).building a tailored dataset of active molecules with proven inhibition activity against (ABL Proto-Oncogene 1 (ABL1), Proto-oncogene tyrosine-protein kinase Src (SRC), Phosphoinositide 3-kinases (PI3Ks), mammalian target of rapamycin (mTOR), and AKT Kinase) from publicly available databases, 2) ensemble docking (FLARE), 3) ADME evaluation, 4) molecular dynamics (FLARE). The results obtained in our study for the first time could identify drug like multi-kinase allosteric inhibitors with diverse heterocycle scaffolds (Purine, Pyrimidine, Pyridine, Piperazine, Benzimidazole, Pyrazole, and benzotriazole) with potential binding affinity to EGFR L858R/T790M/C797S and one of the network kinases. Key residue contacts specific to the heterocycle scaffold were identified. These novel putative allosteric multi-kinase inhibitors stand a good chance of being tested in NSCLC patients either individually or in a combination of orthosteric/ chemotherapeutic agents to overcome resistance and toxic side effects after experimental studies. This discovery of promising scaffolds will boost research in future multi-kinase allosteric drug discoveries.

KEYWORDS

allosteric; multi-kinase; EGFR; non-small cell lung cancer (NSCLC); molecular docking; heterocyclic scaffold

INTRODUCTION

According to the World Health Organization, lung cancer is the second most recurrent type of cancer in the world, with a high mortality rate compared to other malignancies. (https://www.who.int/news-room/fact-sheets/detail/cancer). Non-small cell lung cancer (NSCLC) is the most frequent type of lung cancer (80-85% of cases) with a poor prognosis [1]. Epidermal growth factor receptor (EGFR) is the most prospective therapeutic oncogenic target in lung cancer, its overexpression is observed in more than 60% of patients with metastasis. At molecular level, drug resistance for first, second and third generation of anti EGFR drugs was correlated to the activating mutations (T790M and C797S) at the drug binding site or conventional ATP binding site [2,3]. Subsequently, fourth-generation NSCLC drugs such as EAI001, EAI045, JBJ-04-125-02, and DDC4002 were developed, which bind to the allosteric site of EGFR, inhibiting cell proliferation and arresting EGFR L858R/T790M/C797S signalling [4,5,6]. Although allosteric drugs have few negative effects, they have low oral bioavailability and drug retention over long-term administration. [7,8]. Thus, there is a pressing need to identify potential anti-NSCLC compounds using novel approaches that take less time yet have a higher possibility of getting approval.

Emerging facts on the complex signalling network activated by the tyrosine kinases highlight the need to incorporate the latest research to develop successful EGFR-targeting therapeutics. It has already been demonstrated that uncontrolled EGFR activation stimulates multiple downstream pro-oncogenic signalling pathways, including the RAS-RAF-MEK-ERK MAPK and AKT-PI3K-mTOR pathways, along with cellular kinases such as SRC and ABL1. The continuous activation of these molecules/pathways by mutant EGFR causes signal amplification, which promotes unregulated cell division and proliferation, and ultimately causes cancer [9,10,11].

Allosteric inhibition of kinases has resulted in pharmacological effects and clinical benefits comparable to those of orthosteric inhibition. However, the number of kinase targets associated with FDA-approved allosteric drugs is small, highlighting the challenges in identifying and validating allosteric inhibitors [12].

The importance of public and proprietary databases, which contain binding data for hundreds of thousands of active chemicals, was previously emphasised by Narayanan and his colleagues [13]. In this study, a novel approach was designed to identify novel allosteric EGFR $^{L858R/T790M/C797S}$ inhibitors with multi-kinase inhibition potential using in silico methodologies.

MATERIALS AND METHODS

System specifications: Processor Intel (R) Core (TM) i7-10750H CPU @ 2.60GHz, 2.59 GHz, RAM16.0 GB, Nvidia GEFORCE RTX 2070 graphic card was used.

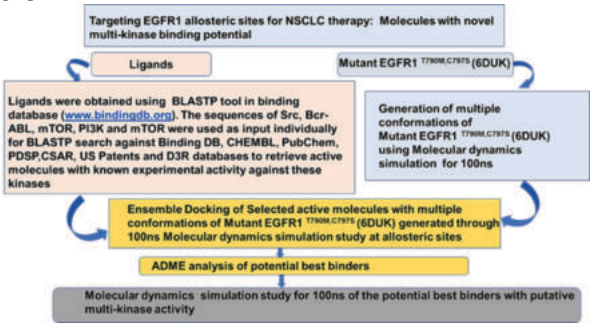

Figure 1. A Schematic Representation Of The Methodology Followed Is Outlined Briefly.

Protein Preparation and generation of mutant EGFR $^{L858R/T790M/C797S}$ (PDB ID: 6DUK) ensemble using Molecular dynamics.

Molecular dynamics simulations in Flare are based on the OpenMM package Flare, version, 2.4, Cresset®, Litlington, Cambridgeshire, UK; http://www.cresset-group.com/flare/ [14,15]. All the molecular dynamics simulations were carried out using the AMBER FF14SB force field [16] together with General Amber Force Field (GAFF) parameters. The crystal structure of the mutant EGFR (PDB ID: 6DUK) complexed with allosteric ligand JBJ-04-125-02 was used as input. The system was explicitly solvated by using the TIP3P water model [17]. The system was modelled using the topology information from the PDB file, the Long-range Coulomb interactions were calculated using the Particle Mesh Ewald (PME) method using a cutoff of 1 nanometre and constrained hydrogen bond length. Later, the system was set for simulation using a Langevin Integrator with a temperature of 300 K and a friction coefficient of 1 ps^{-1}. Both 2 fs and 5 fs integration time stages were used in this study. The system was energy minimised to eliminate clashes, and then the system was simulated for 100 ns. The output was saved to a PDB file every 1000 steps. The structure was written in a DCD file, and the current time, potential energy, and temperature were in a log file (http://openmm.org/documentation.html). The structure corresponding to every 10ns was saved, including the starting structure.

Obtaining ligands from the binding database and ligand preparation.

As kinases share the catalytic domain with similar topology, architecture, and important motifs essential for catalysis, we have used the ligands of ABL, SRC, mTOR, PI3K, and AKT kinases with data on experimental binding affinity from the binding database (https://www.bindingdb.org/bind/info.jsp) for the current study [18]. These ligands were retrieved using the "find compounds for my targets" option through a BLASTP search. The sequence of the respective kinases (ABL, SRC, mTOR, PI3K, and AKT) was searched for matching ligands in the Binding Database: curated from Articles and Patents, CHEMBL extracted from the ChEMBL database, PubChem: extracted from PubChem confirmatory BioAssays, PDSP: PDSP (Psychoactive Drug Screening Program) Drug Database, CSAR: CSAR: extracted from CSAR data, US Patents extracted from US Patents by BindingDB and D3R extracted from D3R database, through BLASTP search using the sequence of ABL, SRC, mTOR, PI3K, and RAC-alpha serine/threonine-protein kinase (AKT). Total of 27529 compounds were obtained in this search for the above-mentioned kinases. These compounds were filtered by removing duplicates, and the ligands that showed >80% human absorption, zero violations of Lipinski's rule of 3, and < 5 Slog P values were selected for further study. Finally, 2998 small molecules were selected for docking against the mutant EGFR structure (PDB ID: 6DUK) (www.rcsb.org) to check their binding affinity. Before using them for docking, all the ligands mentioned in the previous section were further optimized and minimized in Cresset Flare software using default settings [19,20].

Ensemble Docking

Flare software by Cresset was used for molecular docking studies. Docking and scoring in Flare were performed using the Lead Finder docking algorithm [21]. This software assumes protein to be rigid and examines the ligand potential conformations by rotating functional groups around each freely rotatable bond. Lead Finder can pick the best binding molecules using its conformational search algorithm and a high-accuracy scoring function for calculating the free energy of protein-ligand binding. The final set of 2998 molecules were docked with an ensemble of EGFR (6DUK) protein, generated through molecular dynamics simulation for 100 ns. The ensemble of 6DUK structures corresponding to every 10ns of a 100ns trajectory, including the starting conformation obtained through molecular dynamics simulation, was docked against the dataset of 2998 molecules using ensemble docking of Flare with default settings in normal mode. The grid box was defined based on allosteric residues identified in 6DUK [22, 23]. Flare docking includes four major stages. Stage 1 (protein preparation), stage 2 (calculation of an energy grid map for the protein binding site), stage 3 (docking the ligand structures), and stage 4 (the docked poses are scored using Lead Finder's scoring functions). http://www.biomoltech.com/ (Lead Finder, version, BioMolTech®, Toronto, Ontario, Canada; http://www.cresset-group.com/lead-finder/).

Maestro free viewer and Lig plot were used for understanding ligand interactions with the receptor structures (Schrödinger Release 2021-1: Maestro, Schrödinger, LLC, New York, NY, 2021).

SWISS ADME Evaluation

Absorption, Distribution, Metabolism, Excretion/Elimination (ADME) evaluation of the compounds was carried out using Swiss ADME online software [24] (http://swissadme.ch/).

Molecular Dynamics Studies Of Protein-ligand Complex

The methodology used was the same as described for molecular dynamics simulation studies of EGFR above. The potential docked complexes were simulated for a time of 100ns.

RESULTS AND DISCUSSION

Allosteric targeting of EGFR offers a potential alternative for NSCLC patients with L858R/T790M/C797S mutations. Importantly, the diverse location of allosteric sites enables higher selectivity, increases drug sensitivity, lowers toxicity, and improves physicochemical properties. [25]. However, allosteric drugs EAI005 & JBJ-04-125-02 while being effective, showed significant improvement in efficacy in combination with Cetuximab or Osimertinib in lung cancer driven by $EGFR^{L858R/T790M}$ and $EGFR^{L858R/T790M/C797S}$ [5,6]. Furthermore, low oral bioavailability and drug accumulation on long term treatment [26], the need for the discovery of multi-kinase inhibitors, and the lack of information on diverse putative scaffolds, have set the stage for an urgent need for the discovery of novel allosteric multi-kinase inhibitors for NSCLC.

Targeting proteins whose expression is interconnected was projected to be beneficial in the management of cancer and the suppression of cellular ageing [27,28,29]. The role of SRC, ABL1 and pathway proteins like PI3K, mTOR and AKT in lung cancer signalling is well established [9,10,11]. Therefore, in the study we obtained bioactive molecules of ABL, SRC, mTOR, PI3K, and RAC-alpha serine/threonine-protein kinase (AKT) from binding database, CHEMBL, PubChem other databases with experimentally proven active molecules (section 2.2), to study their binding affinity with mutated EGFR as these databases were proposed to provide a good starting point for lead optimization and drug repurposing studies [13].

An ensemble of EGFR structure bound to allosteric inhibitor JBJ-04-125-02 (6DUK) was generated using molecular dynamics methods as it was proposed to be useful for proteins whose ligand binding space is not well known and to incorporate dynamic aspects of protein-ligand binding and thermal protein fluctuations resulting in exposure of different binding sites [30, 31,32,33]. The EGFR conformations thus obtained were extracted at the interval of 10ns, as clustering the trajectories of molecular dynamics does not always identify the protein conformations that ligands favour [34]. Molecular docking was proved to be useful in predicting the kinase and anticancer inhibitors [35] thus ensemble docking with selected dataset of 2998 ligands was performed using Flare software (FLARE. 2.4 Flare, version, Cresset®, Litlington, Cambridgeshire, UK; http://www.cresset-group.com/flare/) is based on the Lead Finder algorithm [21] (supplementary material S1, S2, S3.csv).

154 potential ligands were chosen from the docking results based on: Binding conformation of the potential ligand within the allosteric site comparable to the allosteric inhibitor JBJ-04-125-02, LF rank score of >= -8 Kcal/ mole in the docked complex of all EGFR conformations, LF score between -15 to -12 Kcal/mol in the best docked pose, (Supplementary material S4.csv). The LF rank score is an indicator of the binding affinity of the protein-ligand complex. The more negative the LF rank value is, the stronger is the ligand's affinity for the EGFR triple mutant structure (6DUK) [21]. The Flare docking algorithm was validated by re-docking crystallized JBJ-04-125-02 to the crystal structure 6DUK (Supplementary material: Figure S1). Although the docking score by itself does not give a precise estimate of binding, it can be used to evaluate potential ligands when validated with successful self-docking data [36,37]. The SwissADME analysis of six physicochemical properties (lipophilicity: XLOGP3 between −0.7 and +5.0, size: MW between 150 and 500 g/mol, polarity: TPSA between 20 and 130 Å^2, solubility: log *S* not higher than 6, saturation: fraction of carbons in the sp3 hybridization not less than 0.25, and flexibility: no more than 9 rotatable bonds) depicted by the bioavailability radar resulted in the identification of 29 potential druglike ligands which showed no deviation from the limits of the bioavailability radar [24] (Supplementary material S6 and Table S1 and Figure S2-S8).

The 29 druglike ligands thus obtained showed Purine (3), Pyrimidine (14), Pyridine (3), Piperizine (3), Benzimidazole (1), Pyrazole and Benzotriazole (2) heterocycle scaffold. The ligands BDBM97862 and BDBM97956 have Benzotriazole as primary heterocyclic scaffold. Interestingly, Benzotriazole scaffold was not observed in any of the kinase inhibitors yet [38] (Supplementary material: Table S1, Figure S2-S8). These findings are significant because orthosteric inhibitors have a heterocycle scaffold of Pyrolopyrimidine/ Purine/ Pyrimidine/ Thiazole/ Quinazoline, whereas allosteric inhibitors have only a thiazole heterocycle scaffold. [38].

The investigation of the binding modes of potential allosteric binders yielded some interesting results. Most small molecules with purine as their primary heterocycle interacted with the F723, A722 of the P-loop, and the K749 residue of the loop between the β3 strand and the αC-helix. Based on the proximity of the OH of the phenol group or the NH of the pyrimidine group, the hydrogen bond was observed in smaller molecules with Pyrimidine heterocycles bound to the K745 at the β3 strand. Small molecules with Pyridine heterocycle scaffold shared interactions with β3 residues and αC-helix. Potential binders with Quinazolin heterocycle scaffold displayed hydrogen bonding with E758 at αC-helix. The key interacting residues of different primary heterocycles were as follows (the position of the residues is indicated within brackets). *Purine*- K745 (β3-strand), E749 (loop between β3-

strand and αC-helix), F723 (P-loop), D855 (DFG motif of activation loop), G724 (P-loop), K875 (activation loop), *Pyrimidine*- A722 (P-loop), K875(activation loop), K745(β3-strand), D855 (DFG motif of activation loop), E758 (activation loop), R836 (activation loop), G874 (activation loop), R841 (activation loop), E746 (β3-strand), C775, E748 (β3-strand). *Pyridin*e- E749 (loop between β3 strand and αC-helix). K745 (β3-strand), E758 (αC-helix) L861. *Piperazine* A755 & E758 (αC-helix). *Benzimidazol* -A722 (P-loop). *Pyrazole*- K745 (β3 strand). In this study, we have also identified a novel heterocycle scaffold with Benzotriazole scaffold as the primary heterocycle (dimethylamino)ethyl]-4-[[7-(2,6-dimethylphenyl)-5-methyl-1,2,4-benzotriazin-3-yl], as there are no kinase inhibitors known with Benzotriazole scaffold as primary heterocycle. The amino group of the dimethylamino group interacts with E749 present on the β3-αC-helix loop that connects the αC-helix and β3-strand. According to a recent report, the conserved β-3 strand lysine of protein kinases acts as an integrator node to coordinate the allosteric coupling of the two ligand-binding sites. It maintains indirect ATP-pocket interactions and mediates a critical salt bridge with a glutamate (Glu130) of the αC-helix that is conserved across all kinases [39]. It is important to note that the K745 β-3 strand was identified as one of the key residues for ligand binding in this study, the other residues were E746, E748, E749, A755, E758, A722, F723, R836, L861 and K875 respectively in various conformations of EGFR (6DUK) (Supplementary material: Figure S2-S8; Table S1). Targeting these residues may be useful in developing new allosteric multi-kinase kinase inhibitors Molecular dynamics simulation study was conducted with complex of EGFR-with BDBM50315757 (Inhibitor of Serine/threonine-protein kinase mTOR), BDBM97862-(inhibitor of SRC Kinase), BDBM50331590 (inhibitor of Phosphatidylinositol 4,5-bisphosphate3-kinase catalytic subunit alpha isoform) and, BDBM50256383 (AKT Inhibitor which showed promising binding affinity). During the simulation period of 100ns, information on RMSD, potential energy and the percentage of contacts were derived. Molecular dynamics simulation studies of EGFR(6DUK)-50315757 complex showed stable interaction of ligand within the binding site as depicted by equilibrated RMSD (Figure 3,4,5,6).

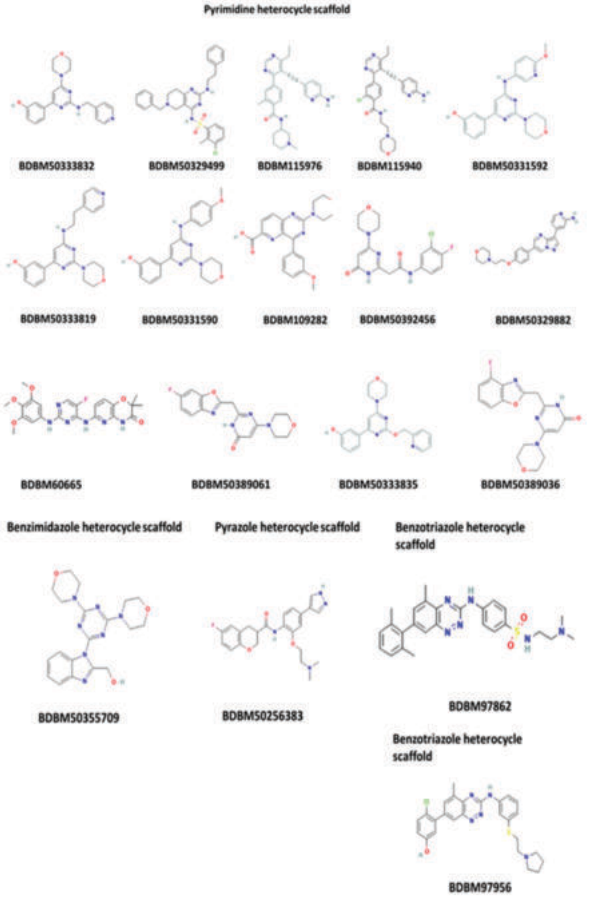

Figure 2. The Structures Of Potential Multi-kinase Allosteric Binders Of Mutant EGFR(6DUK).

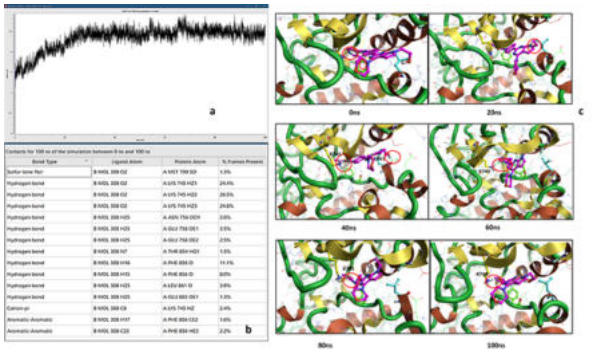

Figure 3. Molecular dynamics simulation study of EGFR (6DUK)-BDBM5031757 complex. a)The molecular dynamics simulation shows a gradual increase in the RMSD value with fluctuations, stabilizing at an average of 2.7□ Å. b) Contact percentage of various interactions between EGFR and 6DUK in various frames during the entire period of simulation is shown. c) Hydrogen bonding interaction of contact residues of EGFR (6DUK) complexed with the ligand 50315757 during entire trajectory of 100ns.

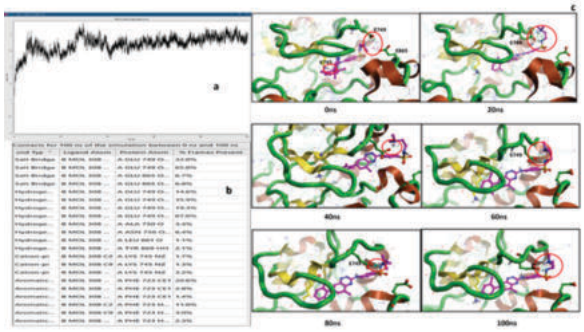

Figure 4. Molecular dynamics simulation study of EGFR (6DUK)-BDBM-97862. The molecular dynamics simulation shows a gradual increase in the RMSD value with fluctuations, stabilizing at an average of 2.7□Å. b) Contact percentage of various interactions between EGFR and 6DUK in various frames during the entire period of simulation. c) Hydrogen bonding interaction of contact residues of EGFR (6DUK)-97862 (complex) during the entire trajectory of 100ns.

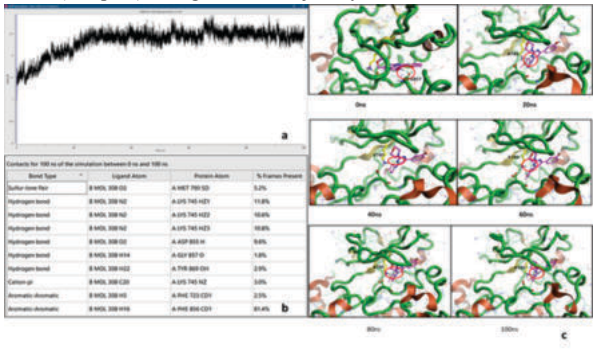

Figure 5. Molecular dynamics simulation study of EGFR (6DUK)-BDBM-50331590 complex. a) The molecular dynamics simulation shows a gradual increase in the RMSD value with fluctuations, stabilizing at an an average of 2.1□ Å. b) Contact percentage of various interactions between EGFR and 6DUK in various frames during the entire period of simulation is shown. c) Hydrogen bonding interaction of contact residues of EGFR (6DUK)-50331590 complex during the entire trajectory of 100ns

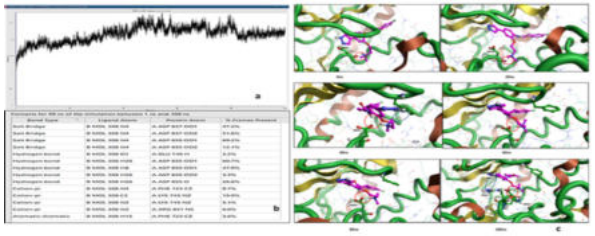

Figure 6. Molecular dynamics simulation study of EGFR(6DUK)-

BDBM50256383 complex. The molecular dynamics simulation shows a gradual increase in the RMSD value with fluctuations, stabilizing at an average of 2.2□ Å. b) Contact percentage of various interactions between EGFR (6DUK) complexed with 50256383 in various frames during the entire period of simulation is shown. c) Hydrogen bonding interaction of contact residues of EGFR (6DUK) - 50333835 complex during entire trajectory of 100ns.

Further, analysis of EGFR -BDBM5031757 docked complex during 100ns simulation period led to following observations: The ligand was stabilized mainly by hydrogen bond interaction with K745 (>50% of frames) and with also with N756, E758 and F856 in a few frames. (Figure S3b & c, supplementary material M1.mp4). Hydroxy ethyl group of the 1-[4-[7-(2-hydroxyethyl) -4-morpholin-4-ylpyrrolo [2,3-d] pyrimidin-2-yl] phenyl] -3-pyridin-4-ylurea was positioned towards the loop β3-αC-helix loop that connects the αC-helix and β-strand (β3) and was flexible making interactions with activation loop or loop between β3 and αC- helix. The P-loop showed variation in shape from curved to kinked structure. However, K745 residue was in constant interaction with OH group of Urea group. F856 aromatic - aromatic interaction was seen between pyridine ring (Figure 3c, Supplementary material M1.mp4). EGFR- 97862 docked complex showed hydrogen bonding interaction with E749. While the residue E749 was engaged in hydrogen bonding interaction (>90% of frames) and salt bridge interaction (>65% of frames) during most of the simulation period, the residues N756 and E865 showed hydrogen bond interaction and salt bridge interactions N756 sparingly (6.5% & 6.8% of frames) (Figure 4b). The amino group of dimethylamino group of the ligand showed hydrogen bonding interaction with the E749 (β3-αC-helix loop that connects the αC-helix and β-strand (β3) (>90% of the frames) or salt bridge interaction (>65% of the frames) during the simulation period. F723 (P-loop) was seen to involve in aromatic-aromatic interaction (32% of the frames). The residue E749 present in the β3-αC-helix loop that connects the αC-helix and β-strand (β3) was engaged in contact during the entire trajectory and was aligned parallel towards αC-helix which is in out configuration in the 6DUK crystal structure (Figure 4c, M2.mp4). The pose of the EGFR- 50331590 complex showed hydrogen bonding interaction with K745 and G857, while the residue K745 followed by D855 was engaged in hydrogen bonding interaction during most of the simulation period. While the residue F856 was engaged in aromatic- aromatic residue interaction with the ligand (81.4% of frames). Analysis of the binding pose of the complex frame every 20ns in 100ns time frame showed that the position of the ligand oscillated between the DGF motif of the activation loop and K745 of the β3 strand. The methoxy group and the pyrimidine group of ligands displayed hydrogen bonds with D855 and K745 respectively (Figure 5b & c, Supplementary material M3.mp4). The analysis of contacts between EGFR (6DUK) complexed with the ligand 50256383, showed that hydrogen bonding interaction with residues D837 (>50% of frames) and D855 (>65% of frames). K745 showed cation-π interaction in 55% of frames of the time during the 100ns simulation period (The ligand was positioned towards the activation loop near the DFG group and the residue D855 (80% of the frames) and D837 (> 50% of the frames) played a major role in holding the ligand in the allosteric cavity. The binding contact of D855 with an amino group of dimethylamino group was retained throughout the 100ns of simulation time (Figure 6b & c, Supplementary material M4.mp4.

Allosteric Multi-kinase therapy appears to be the next step forward in lung cancer care. This can apply not only to molecules that work independently to inhibit multiple pathways but also to combinations of therapies that act in concert to inhibit malignant growth by targeting multiple pathways [39]. Since these inhibitors identified in the present study were discovered as competitive inhibitors of their respective kinase families in the lab, the hypothesis of blocking both orthosteric and allosteric sites using them could become a possibility as bidirectional and synergistic allosteric propagation in collaborative, dual-liganded enzyme targets provides a strategy for combinatorial drug design and therapy [38].

CONCLUSION

The current allosteric inhibitors of mutant EGFR are dominated by thiazole heterocycle scaffold. In this investigation, small molecule allosteric inhibitors binding triple mutant EGFR having diverse heterocycle scaffolds (Pyrimidine, Purines, Pyridines, Piperazine, Pyrazole, Benzimidazole, and a unique Benzotriazole scaffold not previously reported in any of the kinase inhibitors) were identified. The ligands obtained from the present are reasonably diverse and suggest the possible chemical space in allosteric drug discovery which is dominated by a thiazole heterocycle scaffold. Many allosteric kinase inhibitors with improved predicted activity and binding affinities against EGFR could be designed using *in silico* modification of these scaffolds, which could serve as lead compounds for experimental validation, and further preclinical testing.

Declarations

Funding: The corresponding author is pleased to acknowledge the department of science & technology, Government of India for financial support vide reference no SR/LS310/2017 under Women Scientist Scheme to carry out this work.

Conflicts Of Interest/ Competing Interests: None.

Declaration Of Competing Interest: None

Acknowledgements:

The corresponding author is pleased to acknowledge the department of science & technology, Government of India for financial support vide reference no SR/LS310/2017 under Women Scientist Scheme to carry out this work. The authors would like to thank Cresset for providing the software to carry out this work. The authors would also like to thank Prof. P.P. Reddy, the Research Director at Bhagwan Mahavir Medical Research Centre, as well as the Management, for their ongoing encouragement and support.

Link To Supplementary Material.

https://drive.google.com/drive/folders/12x3f8I3PR_2jv4mLjGfpJxjOaaFH9ku?usp=sharing ;https://docs.google.com/document/d/1Rw8HdKO6pK6fVapIHLi39Q5wrwv_ZyI0/edit?usp=sharing&ouid=113618202846385339529&rtpof=true&sd=true https://docs.google.com/document/d/19lHX69wA0UCuF7lctzMyI8KcNOgJKDX/edit?usp=sharing& ouid=113618202846385339529&rtpof=true&sd=true

REFERENCES

1. Bray F, Ferlay J, Soerjomataram I, Siegel RL, Torre LA, Jemal A. Global cancer statistics 2018: GLOBOCAN estimates of incidence and mortality worldwide for 36 cancers in 185 countries. CA Cancer J Clin. 2018;6:394-424. doi: 10.3322/caac.21492. Epub 2018 Sep 12. Erratum in: CA Cancer J Clin. 2020; 4:313.
2. Kim MK, Yee J, Cho YS, Jang HW, Han JM, Gwak HS. Risk factors for erlotinib-induced hepatotoxicity: a retrospective follow-up study. BMC Cancer. 2018;1:988. doi: 10.1186/s12885-018-4891-7.
3. Zhang Y, Wang C, Liu Z, Mang Q, Huo X, Liu Q, et al. P-gp is involved in the intestinal absorption and biliary excreation afatinib in vitro and in rats. Pharmacol Rep. 2018;2:243–250. doi: 10.1016/j.pharep.2017.10.005.
4. Fassunke J, Müller F, Keul M, Michels S, Dammert MA, Schmitt A, Plenker D, Lategahn J, Heydt C, Brägelmann J, Tumbrink HL, Alber Y, Klein S, Heimsoeth A, Dahmen I, Fischer RN, Scheffler M, Ihle MA, Priesner V, Scheel AH, Wagener S, Kron A, Frank K, Garbert K, Persigehl T, Püsken M, Haneder S, Schaaf B, Rodermann E, Engel-Riedel W, Felip E, Smit EF, Merkelbach-Bruse S, Reinhardt HC, Kast SM, Wolf J, Rauh D, Büttner R, Sos ML. Overcoming EGFRG724S-mediated osimertinib resistance through unique binding characteristics of second-generation EGFR inhibitors. Nat Commun. 2018; 9 :4655. doi: 10.1038/s41467-018-07078-0.
5. Jia Y, Yun C, Park E, Ercan D, Manuia M, Juarez J, et al. Overcoming EGFR(T790M) and EGFR(C797S) resistance with mutant-selective allosteric inhibitors. Nature. 2016; 534:129–132. doi: 10.1038/nature17960.
6. Zhao P, Yao MY, Zhu SJ, Chen JY, Yun CH. Crystal structure of EGFR T790M/C797S/V948R in complex with EAI045. Biochem Biophys Res Commun. 2018; 502:332–337. doi: 10.1016/j.bbrc.2018.05.154.
7. To C, Jang J, Chen T, Park E, Mushajiang M, De Clercq DJH, et al. Single and dual targeting of mutant EGFR with an allosteric inhibitor. Cancer Discov. 2019; 9:926–943. doi: 10.1158/2159-8290.CD-18-0903.
8. De Clercq DJH, Heppner DE, To C, Jang J, Park E, Yun CH, et al. Discovery and optimization of dibenzodiazepinones as allosteric mutant-selective EGFR inhibitors. ACS Med Chem Lett. 2019;10:1549–1553. doi: 10.1021/acsmedchemlett.9b00381.
9. Belli S, Esposito D, Servetto A, Pesapane A, Formisano L, Bianco R. c-Src and EGFR Inhibition in Molecular Cancer Therapy: What Else Can We Improve? Cancers (Basel). 2020;12:1489. doi: 10.3390/cancers12061489.
10. Watanabe K, Kage H, Nagoshi S, Toyama K, Ohno Y, Shinozaki-Ushiku A, Nakazaki K, Suzuki H, Kurokawa M, Nagase T. Dual EGFR and ABL Tyrosine Kinase Inhibitor Treatment in a Patient with Concomitant EGFR-Mutated Lung Adenocarcinoma and BCR-ABL1-Positive CML. Case Rep Oncol Med. 2020; 2020:4201727. doi: 10.1155/2020/4201727.
11. Fang W, Huang Y, Gu W, Gan J, Wang W, Zhang S, Wang K, Zhan J, Yang Y, Huang Y, Zhao H, Zhang L. PI3K-AKT-mTOR pathway alterations in advanced NSCLC patients after progression on EGFR-TKI and clinical response to EGFR-TKI plus everolimus combination therapy. Transl Lung Cancer Res. 2020; 9(4):1258-1267. doi: 10.21037/tlcr-20-141.
12. Brognard J, Clark AS, Ni Y, Dennis PA. Akt/protein kinase B is constitutively active in non-small cell lung cancer cells and promotes cellular survival and resistance to chemotherapy and radiation. Cancer Res. 2001; 61:3986-97.
13. Pan Y, Mader MM. Principles of Kinase Allosteric Inhibition and Pocket Validation. J Med Chem. 2022. doi: 10.1021/acs.jmedchem.2c00073. Epub ahead of print.
14. Narayanan D, Gani OABSM, Gruber FXE, Engh RA. Data driven polypharmacological drug design for lung cancer: analyses for targeting ALK, MET, and EGFR. J Cheminform. 2017; 9:43. doi: 10.1186/s13321-017-0229-8.
15. Kuhn M, Firth-Clark S, Tosco P, Mey ASJS, Mackey M, Michel J. Assessment of Binding Affinity via Alchemical Free-Energy Calculations. J Chem Inf Model. 2020; 60:3120-3130. doi: 10.1021/acs.jcim.0c00165. Epub 2020 Jun 3.
16. Eastman P, Swails J, Chodera JD, McGibbon RT, Zhao Y, Beauchamp KA, Wang LP,

Simmonett AC, Harrigan MP, Stern CD, Wiewiora RP, Brooks BR, Pande VS. OpenMM 7: Rapid development of high-performance algorithms for molecular dynamics. PLoS Comput Biol. 2017;13:e1005659. doi: 10.1371/journal.pcbi.1005659.
17. Case DA, Abin VB, Berryman JT, Betz RM, Cai Q, Cerutti DS, Cheatham TEI, Darden TA, Duke RE, Gohlke H, Goetz AW, Gusarov S, Homeyer N, Janowski P, Kaus J, Kolossváry I, Kovalenko A, Lee TS, LeGrand S, Luchko T, Luo R , Madej B, Merz KM, Paesani F, Roe DR, Roitberg A, Sagui C, Salomon-Ferrer R, Seabra G, Simmerling CL, Smith W, Swails J, Walker RC, Wang J, Wolf RM, Wu X, Kollman PA (2014) *AMBER 14*, University of California: San Francisco, CA.
18. Price DJ, Brooks CL 3rd (2004) A modified TIP3P water potential for simulation with ewald summation. J Chem Phys. 121:10096–10103.
19. Chen X, Liu M, Gilson MK. BindingDB: a web-accessible molecular recognition database. Comb Chem High Throughput Screen. 2001; 4:719-25.
20. Mehler EL.Self-Consistent, Free Energy Based Approximation To Calculate pH Dependent Electrostatic Effects in Proteins. J Phys Chem. 1996; 100:16006-16018.
21. Mehler EL,Guarnieri F. A self-consistent, microenvironment modulated screened coulomb potential approximation to calculate pH-dependent electrostatic effects in proteins. Biophys J.1999,77:3-22.
22. Stroganov OV, Novikov FN, Stroylov VS, Kulkov V, Chilov GG. Lead finder: an approach to improve accuracy of protein-ligand docking, binding energy estimation, and virtual screening. J Chem Inf Model. 2008;48:2371-2385.
23. Cheeseright T, Mackey M, Rose S, Vinter A. Molecular field extrema as descriptors of biological activity: definition and validation. J Chem Inf Model. 2006;46:665-676.
24. Bauer MR, Mackey MD. Electrostatic Complementarity as a Fast and Effective Tool to Optimize Binding and Selectivity of Protein-Ligand Complexes. J Med Chem. 2019 ;62:3036-3050. doi: 10.1021/acs.jmedchem.8b01925. Epub 2019 Mar 13.
25. Daina A, Michielin O, Zoete V. SwissADME: a free web tool to evaluate pharmacokinetics, drug-likeness and medicinal chemistry friendliness of small molecules. Sci Rep. 2017; 7:42717. doi: 10.1038/srep42717. PMID: 28256516; PMCID: PMC5335600.
26. Zhang J, & Nussinov, R. Protein allostery in drug discovery. Springer Nature 2019.
27. Caporuscio F, Tinivella A, Restelli V, Semrau MS, Pinzi L, Storici P, et al. Identification of small-molecule EGFR allosteric inhibitors by high-throughput docking. Future Med Chem. 2018; 10:1545–1553. doi: 10.4155/fmc-2018-0063. [
28. Gazdar AF, Shigematsu H, Herz J, Minna JD. Mutations and addiction to EGFR: the Achilles 'heal' of lung cancers? Trends Mol Med. 2004;10:481-486.
29. Steelman LS, Chappell WH, Abrams SL, Kempf RC, Long J, Laidler P, Mijatovic S, Maksimovic-Ivanic D, Stivala F, Mazzarino MC, Donia M, Fagone P, Malaponte G, Nicoletti F, Libra M, Milella M, Tafuri A, Bonati A, Bäsecke J, Cocco L, Evangelisti C, Martelli AM, Montalto G, Cervello M, McCubrey JA. Roles of the Raf/MEK/ERK and PI3K/PTEN/Akt/mTOR pathways in controlling growth and sensitivity to therapy-implications for cancer and aging. Aging (Albany NY). 2011; 3:192-222.
30. Mendoza MC, Er EE, Blenis J. The Ras-ERK and PI3K-mTOR pathways: cross-talk and compensation. Trends Biochem Sci. 2011; 36:320-328.
31. Huang SY, Zou X. Ensemble docking of multiple protein structures: considering protein structural variations in molecular docking. Proteins. 2007; 66:399-421.
32. Knegtel RM, Kuntz ID, Oshiro CM. Molecular docking to ensembles of protein structures. J Mol Biol. 1997; 266:424-440. doi: 10.1006/jmbi.1996.0776.
33. Pagadala NS, Syed K, Tuszynski J. Software for molecular docking: a review. Biophys Rev. 2017; 9:91-102. doi: 10.1007/s12551-016-0247-1. Epub 2017 Jan 16.
34. Evangelista Falcon W, Ellingson SR, Smith JC, Baudry J. Ensemble Docking in Drug Discovery: How Many Protein Configurations from Molecular Dynamics Simulations are Needed To Reproduce Known Ligand Binding? J Phys Chem B. 2019;123:5189-5195. doi: 10.1021/acs.jpcb.8b11491. Epub 2019 Feb 12.
35. Wieduwilt MJ, Moasser MM. The epidermal growth factor receptor family: biology driving targeted therapeutics. Cell Mol Life Sci. 2008;65:1566-1584. doi: 10.1007/s00018-008-7440-8.
36. Gagic Z, Ruzic D, Djokovic N, Djikic T, Nikolic K. *In silico* Methods for Design of Kinase Inhibitors as Anticancer Drugs. Front Chem. 2020; 7:873. doi: 10.3389/fchem.2019.00873.
37. Ramírez D, Caballero J. Is It Reliable to Take the Molecular Docking Top Scoring Position as the Best Solution without Considering Available Structural Data? Molecules. 2018 ;23:1038. doi: 10.3390/molecules23051038.
38. Ghode A, Gross LZF, Tee WV, Guarnera E, Berezovsky IN, Biondi RM, Anand GS. Synergistic Allostery in Multiligand-Protein Interactions. Biophys J. 2020;119:1833-1848. doi: 10.1016/j.bpj.2020.09.019. Epub 2020 Sep 28.
39. Haddad Y, Remes M, Adam V, Heger Z. Toward structure-based drug design against the epidermal growth factor receptor (EGFR). Drug Discov Today. 2021; 26:289-295. doi: 10.1016/j.drudis.2020.10.007. Epub 2020 Oct 17.
40. Ghode A, Gross LZF, Tee WV, Guarnera E, Berezovsky IN, Biondi RM, Anand GS. Synergistic Allostery in Multiligand-Protein Interactions. Biophys J. 2020 ;119:1833-1848. doi: 10.1016/j.bpj.2020.09.019. Epub 2020 Sep 28.
41. Bar J, Herbst RS, Onn A. Multi-kinase inhibitors in lung cancer: new clinical data. Clin Lung Cancer. 2008; 9:S92-99. doi: 10.3816/CLC.2008.s.014.